Left-handed materials composed of only S-shaped resonators

Hongsheng Chen, Lixin Ran, Jiangtao Huangfu, Xianmin Zhang, and Kangsheng Chen

Department of Information and Electronic Engineering, Zhejiang University, Hangzhou 310027, China
and Electromagnetics Academy at Zhejiang University, Zhejiang University, Hangzhou 310027, China

Tomasz M. Grzegorczyk and Jin Au Kong

Research Laboratory of Electronics, Massachusetts Institute of Technology, Cambridge, Massachusetts 02139, USA
and Electromagnetics Academy at Zhejiang University, Zhejiang University, Hangzhou 310027, China

We analyze an S-shaped inclusion for the realization of metamaterials exhibiting left-handed properties. Unlike most of the conventional inclusions used so far that are composed of two separate geometries— typically a split ring and a rod—the inclusion proposed in this paper is made of only one S-shaped element which yields an overlapping negative permittivity and negative permeability response over a frequency band of about 2.6 GHz. By adopting this geometry, we manage to lower the negative permittivity frequency band down to the level of the negative permeability frequency band, thus allowing the overlapping to occur. Therefore, the structure works as a stand alone and does not require the use of an additional rod. A theoretical analysis is carried out to study this inclusion and numerical simulations, as well as a Snell refraction experiment, clearly show that the material indeed exhibits a negative index of refraction at some frequencies. The simple pattern of the inclusion, the wide left-handed frequency band exhibited, and the low losses measured indicate the superiority of this inclusion in the realization of left-handed metamaterials.

I. INTRODUCTION

In 1968, Veselago theoretically investigated materials with simultaneously negative permittivity and permeability, or left-handed materials (LHMs), and pointed out that the Snell's law, the Doppler shift, and the Cherenkov radiation are reversed [1]. At microwave frequency, the negative index of refraction was experimentally verified [2] with LHMs realized from a periodic arrangement of metallic printed lines (or rods) that exhibit a negative permittivity [3,4], and a periodic array of split-ring resonators (SRRs) that exhibit a negative permeability [5]. Controversy immediately followed concerning the fundamental issue of whether the negative refraction phenomena associated with a LHM can physically exist [6]. Rebuttals of such theoretical issues were addressed [7,8] and more experimental works were reported [9–11]. The realization of most of the left-handed materials in these experimental works relies on these SRR and rod geometries [2,9,10]. However, it should be noted that the SRRs themselves also exhibit a frequency band of negative permittivity, higher than that of negative permeability, and both do not overlap in general.

In this paper, we propose a design of SRR for which these two frequency bands (corresponding to a negative permittivity and a negative permeability) do overlap in a wide frequency range. This is achieved by properly tuning the geometry of the rings into an S-type structure associated with an inverted image. The theoretical analysis, the numerical simulations and the experimental results confirm the left-handed property of the metamaterial.

II. NUMERICAL ANALYSIS

We begin the analysis by studying the SRR structure shown in Fig. 1(a), where two SRRs are printed on the op-

posite sides of the substrate. The dimensions of the SRR structure are $a=5.2$ mm, $b=2.8$ mm, $h=0.4$ mm, $d=0.5$ mm, and the dielectric constant of the substrate is $\varepsilon_r=1+i0.04$. A unit cell measures 4 mm$\times$2.5 mm$\times$5.4 mm. When a magnetic field is applied, the two capacitances C between the metallic strips enable the induced current to flow around the ring. As it has been shown in [12], this SRR structure can avoid bianisotropy, and has the same magnetic effect as the conventional SRR structures as shown in Fig. 1(b), which were proposed in [2,5,13,14]. The effective permittivity ε_{eff} and permeability μ_{eff} of the structure can be found from the refractive index n and wave impedance z as

$$\varepsilon_{eff}=n/z, \ \mu_{eff}=nz, \tag{1}$$

where n and z can be determined from the measurement of the reflection coefficients and transmission coefficients [15,16] of a wave normally incident on a slab of the metamaterial, followed by the application of a retrieval algorithm [17]. From numerical simulations, the calculated parameters μ_{eff} and ε_{eff} are plotted in Fig. 1(c). We see that the magnetic resonant frequency (ω_{m0}) is at 9 GHz, and the frequency band of negative permeability extends from 9 to 11 GHz. Furthermore, we also see that there exists an electrical resonant frequency (ω_{e0}) at 12 GHz, and the frequency band of negative permittivity is from 12 to 28 GHz. The effective permittivity is strongly dispersive in the vicinity of magnetic resonance and each of the two branches in the ring induces an electrical plasma medium. The electric resonant frequency is introduced by the discontinuity of the two branches. This is further confirmed by the calculated results from a rotated SRR with respect to the incident radiation, as shown in Fig. 1(d). In this case, the magnetic resonance influence on the structure can be neglected, and only an electric resonant fre-
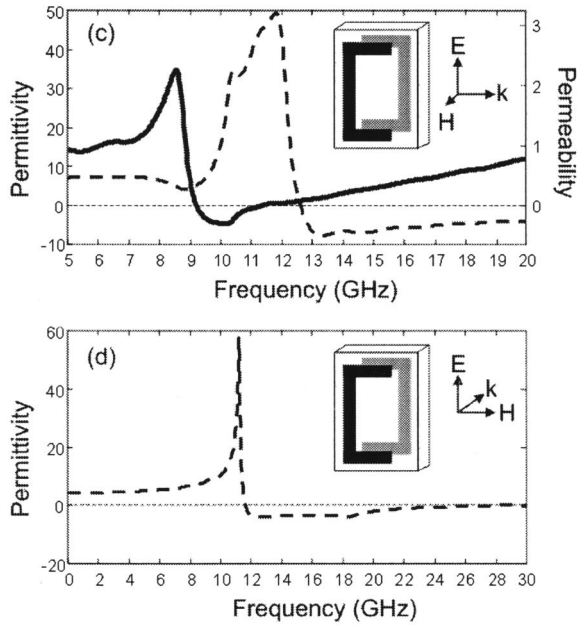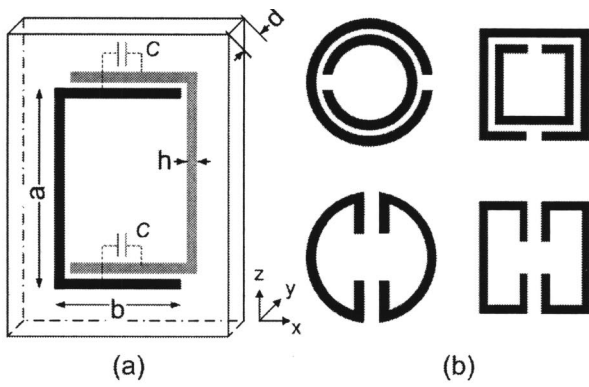
FIG. 1. (a) Simplified ring geometry as first building block toward S structure. Metalizations are reversed on each side of substrate and capacitances C enable current to flow around ring under a magnetic induction. (b) Conventional SRR structures proposed in [2,5,13]. (c) Real parts of permittivity (dashed line, left axis) and permeability (solid line, right axis). (d) Real parts of permittivity. Responses are a function of frequency for SRR structure and incidence shown in inset.
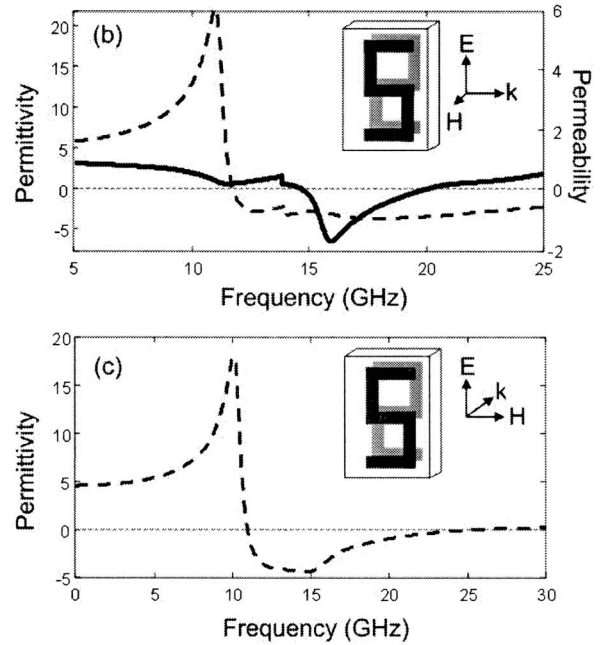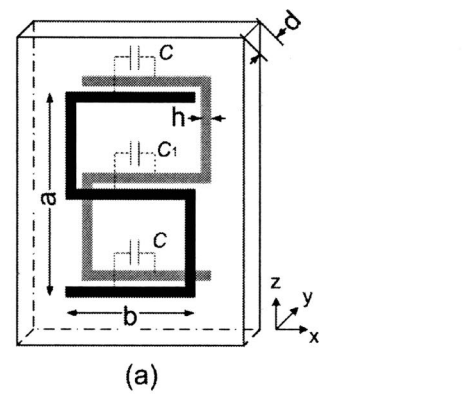

FIG. 2. (a) S-shaped resonator. Note additional capacitance C_1 when compared to Fig. 1(a). (b) Real parts of permittivity (dashed line, left axis) and permeability (solid line, right axis). (c) Real parts of permittivity. Responses are a function of frequency for S-shaped resonator structure and incidence shown in inset.

quency exists. As predicted, the two cases have a similar electric resonant frequency, both around 12 GHz. Thus, we see that for the SRR structure shown in Fig. 1(a), the frequency band of negative permittivity is higher than that of negative permeability and both of them do not overlap. The analysis on the other SRR structures, as shown in Fig. 1(b), yields similar results. The results for the top two insets in Fig. 1(b) are a little different: besides the frequency band of negative permittivity, which is higher than that of negative permeability, there also exists a narrow frequency band of negative permittivity just near the magnetic resonance [18] because of the bianisotropy in these two structures [12]. However, since we wish to design a structure avoiding bianisotropy and with a wide left-handed frequency band, we disregard this narrow frequency band. Instead, by changing the structure, we manage to lower the electric resonant fre-

quency (ω_{e0}) or increase the magnetic resonant frequency (ω_{m0}) to make the two frequency bands overlapp, as is shown below.

The configuration of SRR is shown in Fig. 2(a), where the branches of a single SRR are shaped like a squared S and two SRRs are printed reverse of each other on each side of the substrate, yielding an eightlike pattern when viewed from top. Thus, besides the two capacitances C between the top and bottom metallic strips, there is another capacitance C_1 between the center of the metallic strips. With the period of a unit cell unchanged and the parameters of the structure as $a=5.2$ mm, $b=2.8$ mm, $h=0.4$ mm, $d=0.5$ mm, we plot in Fig. 2(b) the calculated permeability and permittivity of the S-shaped metamaterial from numerical simulations. We also present in Fig. 2(c) the result in the case of different orientation of the S-shaped resonator with respect to the incident radiation. The results show that the electric resonant fre-
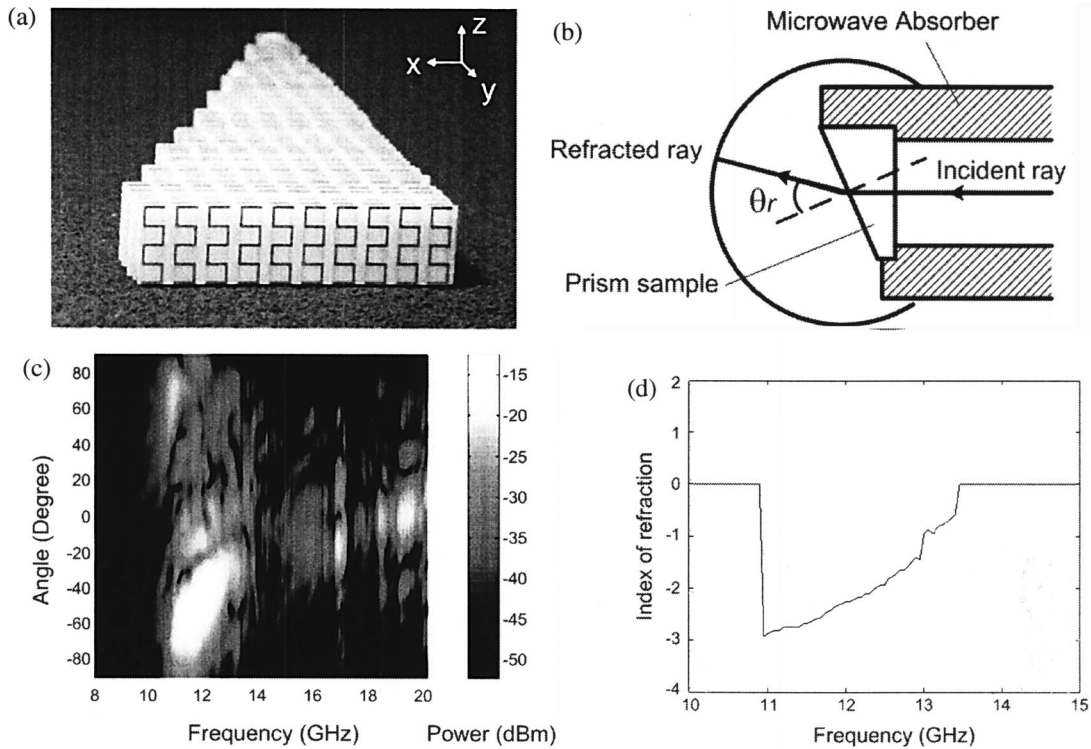
FIG. 3. (a) Sample of prism based on **S** inclusions. (b) Scheme of Snell refraction experimental setup. Sample and microwave absorber were placed between two parallel waveguide plates. (c) Power measured at output of prism as a function of frequency and angle. Metamaterial exhibits a negative refraction index over range from 10.9 to 13.5 GHz. (d) Experimental results of index of refraction vs frequency.

quency ω_{e0}, located at about 11 GHz, is lower than the magnetic resonant frequency ω_{m0}, which occurs at 15 GHz, such that the two frequency bands of negative permittivity and negative permeability overlap from 15 to 20 GHz. We therefore expect the effective index of refraction to be negative within this frequency region.

III. EXPERIMENTAL VERIFICATION

In order to confirm this expected behavior, we have fabricated an **S**-shaped metamaterial sample. A prism as shown in Fig. 3(a) is cut for a Snell refraction experiment. The prism angle is 17.6°. In the sample, the two **S** units are connected to each other to further reduce the electric resonant frequency. The structure has a periodicity of 4 mm along x, 2.1 mm along y, and 10 mm along z. The permittivity of the substrate is $\varepsilon_r=4.6$ and of thickness 1 mm. Compared to the previous section, it is expected that the addition of the dielectric substrate lowers the electric and magnetic resonant frequencies, without otherwise altering the qualitative behavior.

The scheme of the experimental setup is shown in Fig. 3(b), which is very similar to the one reported in [2, Fig. 2]. The experimental results for the Snell refraction experiment are summarized in Fig. 3(c), where the output power measured in far field is shown as function of frequency and output angle. We can extract the index of refraction from these results, which is shown in Fig. 3(d). We see that the metama-

terial has a frequency band of negative refraction from 10.9 to 13.5 GHz (i.e., of about 2.6 GHz).

A transmission experiment for a slab of the metamaterial with 10 unit cells along the incident direction has also been carried out. The results are shown in Fig. 4, where a maximum power of -15 dBm is seen to occur at 12 GHz. We also recorded the transmission power with the metamaterial slab removed and measured a power level of -8 dBm at 12 GHz (data not shown). This indicates that the insertion losses are of -1.75 dB/cm. The losses are significantly less than what we reported with the standard split ring and rod designs [19], which were -6.53 dB/cm. This characteristic, combined with the wide bandwidth, indicates that the metamaterial could be efficiently used in various applications.
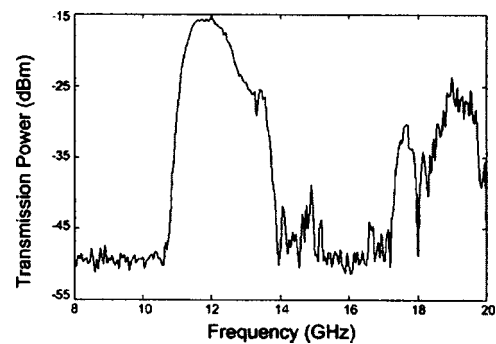

FIG. 4. Experimental results of power transmitted through a 10-unit-cells-long metamaterial vs frequency.
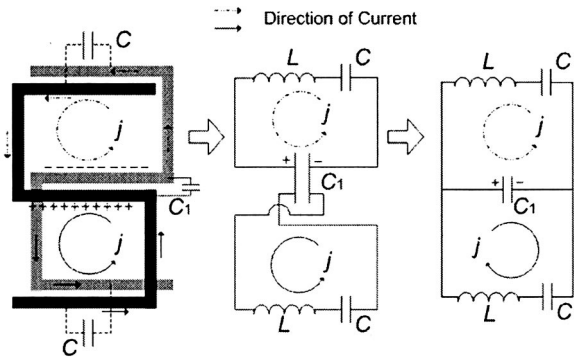
FIG. 5. Equivalent circuit for geometry of Fig. 2(a). Capacitance C_1 enables current to flow in each half ring when a magnetic field is applied.

IV. THEORETICAL ANALYSIS

Both the numerical calculation and experimental results clearly show that the S-shaped SRR yields a metamaterial that exhibits a left-handed behavior. We present here a circuit analysis to show how the S-shaped SRR in Fig. 2(a) resonates and produces a negative permeability.

If the capacitance C_1 does not exist or is very small, it can be treated as an open circuit. In this case, Faraday's law indicates that the total electromotive force around the circumference of the figure-eight pattern (composed of the two opposite S rings) is zero when a time-varying external magnetic field is applied, because the magnetic flux in the top-half and bottom-half area of the figure-eight-pattern structure always cancel each other. However, here C_1 is large and equal to C, so that the existence of C_1 enables the current to flow in each half ring, as shown in Fig. 5. For an inductance L of each half ring directly proportional to the area enclosed by each ring

$$L = \mu_0 (b - 2h) \left(\frac{a - 3h}{2} \right) \approx \mu_0 \frac{ab}{2}, \qquad (2)$$

the circuit theory predicts a resonant frequency equal to

$$\omega_{m0}^{(1)} = \sqrt{\frac{1}{(L/2)(2C/3)}} = \sqrt{\frac{3}{LC}}. \qquad (3)$$

Compared with the SRR structure in Fig. 1(a), we can also get the magnetic resonant frequency to be

$$\omega_{m0}^{(2)} \approx \sqrt{\frac{1}{(2L)(C/2)}} = \sqrt{\frac{1}{LC}}. \qquad (4)$$

We therefore find that the S-shaped SRR in Fig. 2(a) has a magnetic resonant frequency $\sqrt{3}$ times that of the SRR of Fig. 1(a), in agreement with the numerical results which show in Fig. 1(c) that $\omega_{m0}^{(2)} = 9$ GHz and in Fig. 2(b) $\omega_{m0}^{(1)} = 15 \approx 9\sqrt{3}$ GHz.

For the electric properties, the two opposite branches of the S-shaped metallic strip in the structure still behave like a plasma medium when a time-varying electrical field of E_z is applied, and exhibit the same electric property as the conventional SRR of Fig. 1. Yet the extra lengths of wire introduce an extra inductance, and the effect is to decrease the overall plasma frequency [4], allowing the frequency bands of negative permittivity and negative permeability to overlap.

V. CONCLUSION

We have proposed a metamaterial only composed of S-shaped SRRs which, by themselves, i.e., without the need of additional rods, yield metamaterials that exhibit left-handed properties. This conclusion has been verified by numerical simulations, experimental measurements, as well as theoretical calculations. In addition, the left-handed behavior detected has been shown to happen over a wide frequency band (wider than the currently available ones [20]) with very low losses, making the metamaterial a good candidate for various applications.

[1] V. G. Veselago, Sov. Phys. Usp. **10**, 509 (1968).
[2] R. A. Shelby *et al.*, Science **292**, 77 (2001).
[3] J. B. Pendry *et al.*, Phys. Rev. Lett. **76**, 4773 (1996).
[4] J. B. Pendry *et al.*, J. Phys.: Condens. Matter **10**, 4785 (1998).
[5] J. B. Pendry *et al.*, IEEE Trans. Microwave Theory Tech. **47**, 2075 (1999).
[6] P. M. Valanju *et al.*, Phys. Rev. Lett. **88**, 187401 (2002).
[7] J. Pacheco, Jr. *et al.*, Phys. Rev. Lett. **89**, 257401 (2002).
[8] J. B. Pendry *et al.*, Phys. Rev. Lett. **90**, 029703 (2003).
[9] C. G. Parazzoli *et al.*, Phys. Rev. Lett. **90**, 107401 (2003).
[10] A. Houck *et al.*, Phys. Rev. Lett. **90**, 137401 (2003).
[11] J. Huangfu *et al.*, Appl. Phys. Lett. **84**, 9 (2004).

[12] R. Marqués *et al.*, Phys. Rev. B **65**, 144440 (2002).
[13] S. O'Brien and J. B. Pendry, J. Phys.: Condens. Matter **14**, 6383 (2002).
[14] T. M. Grzegorczyk *et al.* (unpublished).
[15] J. A. Kong, Prog. Electromagn. Res. **35**, 1 (2002).
[16] D. R. Smith, S. Schultz, P. Markoš, C. M. Soukoulis, Phys. Rev. B **65**, 195104 (2002).
[17] X. Chen *et al.*, Phys. Rev. E **70**, 016608 (2004).
[18] A. Ishimaru *et al.*, IEEE Trans. Antennas Propag. **51**, 2550 (2003).
[19] L. Ran *et al.*, Chin. Sci. Bull. **48**, 1325 (2003).
[20] L. Ran *et al.*, Phys. Rev. B **70**, 073102 (2004).